agronomy

MDPI

Article

A Comparison of Moment-Independent and Variance-Based Global Sensitivity Analysis Approaches for Wheat Yield Estimation with the Aquacrop-OS Model

Deepak Upreti [1], Stefano Pignatti [2], Simone Pascucci [2], Massimo Tolomio [1], Zhenhai Li [3], Wenjiang Huang [4] and Raffaele Casa [1,*]

1 Dipartimento di Scienze Agrarie e Forestali (DAFNE), Università della Tuscia, Via San Camillo de Lellis, 01100 Viterbo, Italy; dupreti@unitus.it (D.U.); massimo.tolomio@unitus.it (M.T.)
2 Consiglio Nazionale delle Ricerche, Istituto di Metodologie per l'Analisi Ambientale (CNR, IMAA), Via del Fosso del Cavaliere, 100, 00133 Rome, Italy; stefano.pignatti@cnr.it (S.P.); simone.pascucci@cnr.it (S.P.)
3 China National Engineering Research Center for Information Technology in Agriculture (NERCITA), Beijing Research Center for Information Technology in Agriculture, Beijing 100097, China; lizh323@126.com
4 Aerospace Information Research Institute, Chinese Academy of Sciences, Beijing 100094, China; huangwj@aircas.ac.cn
* Correspondence: rcasa@unitus.it

Received: 22 February 2020; Accepted: 20 April 2020; Published: 24 April 2020

Abstract: The present work reports the global sensitivity analysis of the Aquacrop Open Source (AOS) model, which is the open-source version of the original Aquacrop model developed by the Food and Agriculture Organization (FAO). Analysis for identifying the most influential parameters was based on different strategies of global SA, density-based and variance-based, for the wheat crop in two different geographical locations and climates. The main objectives were to distinguish the model's influential and non-influential parameters and to examine the yield output sensitivity. We compared two different methods of global sensitivity analysis: the most commonly used variance-based method, EFAST, and the moment independent density-based PAWN method developed in recent years. We have also identified non-influential parameters using Morris screening method, so to provide an idea of the use of non-influential parameters with a dummy parameter approach. For both the study areas (located in Italy and in China) and climates, a similar set of influential parameters was found, although with varying sensitivity. When compared with different probability distribution functions, the probability distribution function of yield was found to be best approximated by a Generalized Extreme Values distribution with Kolmogorov–Smirnov statistic of 0.030 and lowest Anderson–Darling statistic of 0.164, as compared to normal distribution function with Kolmogorov–Smirnov statistic of 0.122 and Anderson–Darling statistic of 4.099. This indicates that yield output is not normally distributed but has a rather skewed distribution function. In this case, a variance-based approach was not the best choice, and the density-based method performed better. The dummy parameter approach avoids to use a threshold as it is a subjective question; it advances the approach to setting up a threshold and gives an optimal way to set up a threshold and use it to distinguish between influential and non-influential parameters. The highly sensitive parameters to crop yield were specifically canopy and phenological development parameters, parameters that govern biomass/yield production and temperature stress parameters rather than root development and water stress parameters.

Keywords: AOS; Morris; EFAST; PAWN; parameters; density-based

1. Introduction

Crop growth simulation models are important tools for ecology, agriculture and environmental research and management. Such models are used to simulate the behavior of soil-crop systems in response to climate and agriculture management [1–3]. Agricultural processes, the interaction of the crop with the environment and soil over time, are represented by mathematical equations based on theory and empirical research. These equations and parameterizations inevitably entail simplifications of reality, which leads to uncertainty and inaccuracy of output variables [4]. Regardless of the model used, the identification of the parameters and input variables that most affect its output is a fundamental problem for most environmental applications whenever large uncertainty on their values is expected, such as in regional-scale applications [5–7].

In general, crop models contain many parameters and input variables, of which some cannot be measured directly, but can only be inferred by a calibration of the responses observed from the model [8,9]. Manual, one-at-a-time calibration is a very tedious and time-consuming task, which is not feasible for complex models [10]. Numerical optimization or Monte Carlo methods of calibration are widely used [11], but they are prone to errors, e.g., when local minima are present and their efficiency is reduced as the number of parameters increases [12]. Therefore, it is often not possible to include all the parameters in the model calibration [13,14]. In this view, Sensitivity Analysis (SA) is the set of methods that serve the purpose of selecting a limited subset of parameters or input variables, excluding those that are non-influential and have a low impact on the model output. The aim of the SA is to determine how sensitive the outputs of a crop model are with respect to the elements of the model, which are subject to uncertainty or variability [15]. The main purposes of SA are Factor Prioritization (FP) or ranking, Factor Fixing (FF) or screening and Factor Mapping (FM) [16]. This work focuses on ranking and screening.

There are two different strategies for SA: local and global. Local SA focuses on the sensitivity of the factors at particular points in the feature space [17], whereas global SA methods assess the sensitivity in the entire feature space and include higher-order, variance-based methods, e.g., Sobol or Fourier methods [18,19]. An extensive analysis of SA methods on crop models has been performed by different authors [16,20], which shows the inadequacy of local SA methods for crop models due to the complex nature of such models and to the inability to determine the combined effects of the parameters. For these reasons, global SA methods are currently preferred for the SA of the crop models.

Many different global SA methods have been developed [21–25]. Among all these methods, variance-based methods, e.g., Sobol or Fourier, are probably the most widely used for global SA. In general, these methods measure sensitivity to an uncertain parameter or input variable by assessing the contribution of that input to the total variance of the model output variable. The advantage of the variance-based methods is their ability to quantify the contribution of the individual parameters and also quantify the contribution due to interacting effects of the parameters, independently from assumptions on the form of the input–output relation (e.g., linearity and additivity). Variance-based sensitivity indices are also easy to interpret, as they represent the fraction of the output variance caused by the variation of input [26].

Variance-based methods are moment-dependent methods and consider the second-order moment, i.e., variance as a measure of the output uncertainty. It is assumed that this moment is sufficient to describe the output variability [26]. However, it has been recognized that the variance does not adequately represent output uncertainty when the model output is not represented by variance, e.g., output that is highly skewed or multi-modal [25,27,28]. To overcome this limitation (moment-dependent methods), moment-independent global SA measures have been developed [24,25,27]. These methods are also known as density-based methods. They use the entire output distribution to fully characterize the output uncertainty and to quantify the relative influence of the uncertain parameters. The main advantage of these methods, as compared to the variance-based methods, is that they do not use any specific moment of the output distribution to measure the output variability and, therefore, are applicable regardless of its shape (e.g., multi-modal or highly skewed).

The moment-independent density-based Global Sensitivity Analysis (GSA) method, PAWN, was introduced by [25]. It measures sensitivity based on the difference between unconditional output distribution and conditional output distribution, which are obtained simultaneously when all the parameters are free to vary and when one of the parameters is fixed. The difference between PAWN and other density-based methods, e.g., the entropy-based method [27] and the δ-sensitivity measure [24], is that the output distribution in PAWN is characterized by the cumulative distribution function (CDF), whereas in other methods the output distribution is characterized by the probability density function (PDF). The approximation of CDFs by using empirical distributions of the data sample is much easier than the approximation of their PDFs. This facilitates the analysis of the robustness and the convergence of the estimated sensitivity indices [25].

The PAWN method was initially tested with a simple conceptual hydrological model with only five parameters. To further investigate its efficiency, it was applied to the complex environmental model - Soil and Water Assessment Tool (SWAT) [29] with 26 parameters and compared with variance-based method Sobol.

The Aquacrop model [30] is a crop water productivity model developed by the Food and Agriculture Organization (FAO) of the United Nations specifically for the purpose of assessing crop response to water and increasingly used by scientists and agronomists [31–35]. The Aquacrop Open Source (AOS) version was developed by [31] and made available as an open-source Matlab version. In principle, this open-source version is the same as the original developed FAO version of the Aquacrop model. Recently, a version of AOS, v6.0a, has been released. It implements all calculation procedures performed by the original FAO Aquacrop v6.0a, with the exception of soil fertility stress and soil salinity stress, as these are yet to be tested extensively for different crop types and environments worldwide [36]. The soil water balance, stress effects, runoff and plant growth are controlled by a large number of parameters (around 100). Even when some of the parameters can be fixed a priori, calibration of the AOS remains quite challenging, given the relatively large number of parameters (54 in our case) that are typically left to be varied simultaneously. Therefore, SA is often applied prior to the calibration process to identify the most influential parameters and the non-influential ones [7,37]. To avoid any confusion with the model, we will hereafter refer to the FAO developed model as Aquacrop and its open-source Matlab version (The MathWorks Inc., Natick, MA, USA) as AOS that is used in this study.

There have been studies of sensitivity analyses with the FAO developed Aquacrop model [7,37,38], but none yet on the open-source version AOS, which nevertheless lends itself more easily to the integration into regional-scale data assimilation schemes than the standard version. The studies of Aquacrop model SA was based on the arbitrarily chosen thresholds for yield output. According to the authors' best knowledge this is the first time the dummy parameter approach [29] is being used to identify the most influential parameters with the recently released AOS model (v6.0).

The main objectives of this study are to (i) assess and compare the application of the Aquacrop model approach with the Extensive Fourier Amplitude Sensitivity Test (EFAST) method and the density-based PAWN method with a high number of parameters (soil and crop) in terms of parameter ranking results; (ii) perform a sensitivity analysis of the AOS model, provided as an open-source Matlab version, that in principle is similar to the original FAO developed Aquacrop model, but differs in some parameters; (iii) compare the sensitivity indices (SI) of the EFAST and density-based PAWN methods for two different geographical locations and climates. As both methods have different backgrounds and rationale, the comparison cannot be made on the basis of the Sensitivity Index (SI); therefore, the comparison is made in terms of parameter ranking as a measure of the effectiveness with multiple years as a measure of robustness. To assess the parameter ranking, we have used the dummy parameter approach proposed by [29], while the SI of the dummy parameter has used as a threshold to identify non-influential parameters.

2. Materials and Methods

2.1. Sensitivity Analysis

First, the Morris method was used to distinguish between influential and non-influential parameters of the AOS model. The Morris method is designed for an initial screening or the elementary effects that the variation of input factors (parameters and input variables) produces on model outputs. Secondly, the variance-based EFAST method and finally the density-based PAWN method were applied to all the chosen parameters considered for sensitivity analysis (see Table 1), including a dummy parameter to find the higher-order effects and the combined effect of different parameters.

2.1.1. Morris-Based Elementary Effects

The Morris method is designed for the screening of the most influential parameters [39]. It is considered more a qualitative rather than a quantitative method as it does not quantify the sensitivity of a parameter individually, rather it represents the parameter sensitivity in terms of mean (m^*) and sigma (s). High m^* indicates higher sensitivity and higher s indicates interacting effects with other parameters. The method determines whether the effects are negligible, additive, non-linear or the factors are having interacting effects with other parameters [40]. To sample input space, the experimental design is structured in a group of points, called trajectories. In this work, the number of trajectories has been set to 20, which is a value between the minimum suggested by [40] (i.e., 10) and the value used by [37] (i.e., 25) in order to avoid an excessively high computational cost. It computes two indices for each input: the mean of the effects, which measures the total effect of input over the output, and the standard deviation of the effects, which measures the degree of interactions with the other inputs. The input factor with a mean below a threshold value can be considered as having negligible effects on the model output, thus it can be eliminated from further processing by keeping its value as fixed. Whereas, other authors have defined an arbitrary threshold [7,21]. In this work, we chose to identify influential parameters by comparing them with a dummy parameter used as a threshold [29]. All the parameters having a mean value greater than that of the dummy parameter are considered as influential.

2.1.2. EFAST Method

The EFAST method [4] combines the FAST [41] and the Sobol methods [42]. It calculates sensitivity indices using the total variance of the output of the model and the conditional variances depending on the parameters. The interaction among the factors can be quantified by calculating the main SI (Si) and the index of total sensitivity (Sti), i.e., the sum of the main effect plus the interaction between the variation of the terms of the parameters to all orders. Si and Sti range between 0 and 1, with higher values indicating more important effects [7].

In this study, the input parameters plus the dummy parameter were implemented using the EFAST method to identify influential parameters and to rank them. The number of sample points considered for the chosen 55 parameters, including a dummy variable, is 10,000. The required number of runs are thus $55 \times 10{,}000$. The number of higher harmonics M_s is 4, and the number of search curves N_{cs} was set to 1.

2.1.3. Density-Based PAWN Method

The PAWN method is a moment-independent global sensitivity analysis method that takes into account the entire model output distribution for the quantification of the sensitivity of the parameters [25], in comparison to the other variance-based methods that consider only the moments, e.g., the variance of the model output. In general, density-based sensitivity indices measure the sensitivity to parameter x_i by the distance between unconditional PDF and conditional PDF of the model output [24,27]. Practically, PDFs are usually unknown and must be approximated using a data sample. Authors in [25] pointed out the difficulties and limitations of deriving empirical PDFs and suggested to use CDFs instead of PDFs, as it is much easier than using the approximation of PDFs.

In the PAWN method, sensitivity is measured by estimating the variations that are induced in the output distribution when removing the uncertainty about one or more inputs. The sensitivity to the input parameter is measured using the distance between the unconditional probability distribution and the conditional distributions that are obtained by keeping the parameter fixed using the Kolmogorov–Smirnov (KS) statistics [43,44].

The unconditional cumulative distribution function of the model output y is denoted by $F_y(y)$, and the conditional cumulative distribution is denoted by $F_{y|xi}\ (y)$, where x_i is a parameter under consideration.

If $F_y(y)$ and $F_{y|xi}\ (y)$ coincide, it can be concluded that the parameter is non-influential. If the distance between $F_y(y)$ and $F_{y|xi}\ (y)$ is increased, the influence of the parameter increases as well. As a measure between unconditional and conditional CDFs, the *KS* statistics were used (Equation (1) [25])

$$KS\ (x_i) = \max \left| F_y(y) - F_{y|x_i}(y) \right| \quad (1)$$

As *KS* depends on the value at which we fix x_i, the PAWN index T_i considers a statistic (e.g., the maximum or the median) over all possible values of x_i, i.e.,

$$T_i = stat \left| KS\ (x_i) \right| \quad (2)$$

By definition, T_i varies between 0 and 1; the lower the value of $T_{i,}$ the less influential x_i, and if $T_i = 0$, then x_i has no influence on y.

The total number of model evaluations to compute the sensitivity indices are $N_u + n \times N_c \times M$. M is the number of parameters, N_u and N_c are the numbers of unconditional random samples and conditional samples and n is the number of sampling points. In this work, we used $N_u = 300$, $N_c = 200$, $n = 10$ and $M = 55$.

The density-based PAWN method estimates sensitivity by implementing unconditional and conditional cumulative distribution functions. In the case of unconditional distribution functions, all the parameters are free to vary within their defined range, and in the case of the conditional distribution function, the parameter into consideration is fixed to the nominal value. The parameter with the low sensitivity or called PAWN index has the same overlapping unconditional and conditional distribution functions.

In the present study, the Morris and PAWN methods were implemented with the Matlab (The MathWorks Inc., Natick, MA, USA)—based SAFE toolbox [45] and EFAST based on the SA toolbox Eikos [46]. To figure out the best PDF fit for the yield output and different statistical distributions, tests including KS statistics and Anderson–Darling statistics were carried out with EasyFit Evaluation (Ver. 5.6, http://www.mathwave.com/).

2.1.4. Identifying Non-Influential Parameters by Using a Dummy Parameter

Theoretically, the SI of a non-influential parameter is zero. In the case of the PAWN method, SI of zero means that the conditional and unconditional CDF coincides, i.e., fixing the parameter into consideration will have no influence on the model output distribution. The value of zero in the Morris screening test indicates that the parameter has no influence on the model output. However, numerical algorithms and computations are utilized to implement SI, and small but non-zero values can be obtained for non-influential parameters. To set a threshold to identify non-influential parameters, a dummy parameter approach was proposed by [29]. The SI of this dummy parameter provides an indication of the approximation error of the sensitivity analysis. The parameters having SI greater than the SI of the dummy parameter are considered as the influential parameters. It should be noted that the dummy parameter is not added to the model; its SI is calculated by using the sampled data.

2.2. Crop Model: Aquacrop Open Source

Crop growth simulation model Aquacrop was originally developed by the Food and Agriculture Organization (FAO) of the United Nations. As the code of the original model is not accessible, it does not allow, for example, the implementation of data assimilation techniques such as the ensemble Kalman filter, which are increasingly employed for ingesting remote sensing observations into crop models [30]. In this work we have used the open-source Matlab version of the model called Aquacrop Open Source (AOS) developed by [31].

Aquacrop model evolved from the most commonly used empirical approach to assess crop yield response to water [47,48], shown as Equation (3)

$$\frac{Y_x - Y_a}{Y_x} = k_y \left(\frac{ET_x - ET_a}{ET_x} \right) \tag{3}$$

where Y_x and Y_a are the maximum and actual yield, ET_x and ET_a are the maximum and actual evapotranspiration, and k_y is the proportionality factor between relative yield loss and relative reduction in evapotranspiration. The separation of ET into Tr and E avoids the confounding effects of the nonproductive consumption use of water (E), which is important especially during incomplete ground cover, and leads to the conceptual equation at the core of the model [48] (Equation (4), derived by [49]). Yield (Y) as a function of biomass (B) and harvest index (HI) is described as Equation (5):

$$B = WP \times \sum Tr \tag{4}$$

$$Y = B \times HI \tag{5}$$

where Tr is the crop transpiration (in mm), and WP is the water productivity (kg of biomass per m^2 and per mm of cumulated water transpired over the time period in which the biomass is produced), which is a constant for the given climatic condition. By normalizing it for different climatic conditions, WP becomes a conservative parameter [50].

Reference evapotranspiration (ET_0) is provided as a model input: it can easily be estimated using an external calculator [51] that uses the Penman–Monteith equation, following the procedures outlined in FAO Irrigation and Drainage paper no. 56 [52]. The model progressed by separating by evapotranspiration (ET) into crop transpiration (Tr) and soil evaporation (E) using canopy cover (CC). Tr is proportional to the fraction of land surface covered by the canopy, while E is proportional to the surface not covered by the canopy, with some minor adjustments. Tr in the absence of water stress is calculated using the adjusted green canopy cover (CC^*) and the crop coefficient of the full-grown crop, prior to senescence (Kcb), as in Equation (6):

$$Tr = CC^* \times Kcb \times ET_o \tag{6}$$

A distinctive feature of Aquacrop is the use of green canopy cover instead of Leaf Area Index (LAI) to simulate canopy expansion. This allows Aquacrop to be easily used with remote sensing data [48]. Soil evaporation is based on the two-stage Ritchie's approach [53], adopted also in other crop models (e.g., DSSAT crop model).

While the yield–transpiration relationship accounts for the biomass accumulation, canopy expansion and crop phenology are simulated following the thermal time concept, which uses growing degree days (GDDs) as an internal clock of crop development as described in [54], with minor modifications. *CC* development is simulated through a two-stages curve. An exponential equation is used up to half the maximum canopy cover (Equation (7)):

$$CC = CC_0 \times e^{CGC \times t} \tag{7}$$

where *CC* is the fractional canopy cover of soil at time *t*, CC_0 is the initial CC (at time 0) and CGC is the canopy growth coefficient in the percentage of existing *CC* at time *t*. The second half of canopy development follows an exponential decay equation (Equation (8)):

$$CC = CC_x - (CC_x - CC_0) \times e^{-CGC \times t} \tag{8}$$

where CC_x is the maximum canopy cover for optimal conditions. An empirical canopy decline coefficient (*CDC*) is used to characterize the *CC* fractional reduction overtime after maturity has been reached (Equation (9)):

$$CC = CC_x \left[1 - 0.05 \left(exp^{\frac{CDC}{CC_x}} - 1\right)\right] \tag{9}$$

The soil–water balance is simulated first by using the runoff curve number (*CN*) approach of the United States Department of Agriculture (USDA) Soil Conservation Service to separate runoff and infiltration, and then an exponential drainage function is used to simulate downward flow when the soil water content is above field capacity (Equation (10)):

$$\frac{\Delta\theta_i}{\Delta t} = \tau(\theta_{SAT} - \theta_{FC}) \frac{e^{\theta_i - \theta_{FC}} - 1}{e^{\theta_{SAT} - \theta_{FC}} - 1} \tag{10}$$

where θ_i is the actual soil water content, θ_{SAT} is the soil water content at saturation θ_{FC} is the soil water content at field capacity, Δt is the time step (daily) and τ is a coefficient to account for drainage characteristics, derived from the saturated hydraulic conductivity (*Ksat*).

The effect of water-limiting conditions on crop growth is calculated with the ratio of actual available water to total available water *TAW* ($\theta_{SAT\_} \theta_{FC}$) with an approach evolved from the FAO Irrigation and Drainage paper no. 56 [52]. Water stress coefficients (*Ks*) act as modifiers (with values ranging from 0 to 1) of target processes and are used to modulate transpiration, canopy expansion, canopy senescence and pollination when the readily available water (*RAW*) is depleted. *RAW* is defined as a fraction of *TAW* by the *p_up* parameters. Each of the *Ks* coefficients is defined on the basis of the fraction of actual to total available water, using three parameters: the upper threshold (*p_up*, when water stress begins: *Ks* = 1), the lower threshold (*e*, when water stress is complete: *Ks* = 0) and the shape factor of the curve (*fshape_w*).

Extensive descriptions of Aquacrop processes are presented in [30,55]. AOS does not differ in the calculation procedures but is provided as an open-source Matlab version of Aquacrop [31,56]. Test simulations were conducted to verify the suitability of AOS 5.0a to reproduce accurately the calculations and outputs from the original FAO Aquacrop model, considering a range of crop types and environments: wheat production in Tunisia, rice and wheat production in Hyderabad, India, and potato production in Brussels, Belgium. The maximum RMSE and minimum r^2 for crop yields across all simulations were 0.045 t ha^{-1} and 0.993, respectively, which confirms the ability of AOS to reproduce successfully Aquacrop calculations and outputs [56].

Recently, a version of AOS, AOS v6.0a, has been released. AOS v6.0a implements all calculation procedures performed by the original FAO Aquacrop v6.0a model, with the exception of soil fertility stress and soil salinity stress, as these are yet to be tested extensively for different crop types and environments worldwide [36].

There is a total of 89 parameters in the AOS model, as mentioned in the reference manual [57]. Both Aquacrop v6.0a and AOS software include crop files with default parameter values of biomass and canopy growth, thermal time-based phenological stages, transpiration coefficients and temperature and water stresses. In AOS each of these parameters is assigned a specific abbreviation and description in a clearer way with respect to Aquacrop v6.0a. The abbreviations and descriptions of the 54 AOS parameters considered in this work for the SA are listed in Table 1, along with their Aquacrop v6.0a counterparts, as presented in two of the most recent and extensive global SA [58,59]. For clarity, when referring to the previous study, all the parameter abbreviations used in this paper will be written using the AOS notation.

2.3. Setting up the Parameters for AOS Model

In this study, the EFAST and PAWN methods of SA have been applied to the AOS model and compared in terms of parameter ranking. We used all the parameters that were not fixed as mentioned in the AOS manual [57] to be analyzed for SA. The winter wheat grain yield was considered as the output. AOS parameters are reported in Table 1. The range of variation of the selected 54 parameters (reported in Table 1) was determined based on the AOS manual [57] and default values provided with the open-source AOS model database for the wheat crop and also on the previous studies of sensitivity analysis, carried out with the original FAO Aquacrop model [7,37,38]. Since there was no prior information on parameter frequency distributions, they were assumed to have an a priori uniform distribution. It should be noted that [37], in their study, confirms the parameter ranges are more important than their distributions in SA studies.

2.4. Sites Description

In the scenarios applied for the SA test, we used the climate and soil data from two experimental sites. The first site was located in Maccarese (41.833° N, 12.217° E; 8 m a.s.l), western coast of Central Italy, near the Fiumicino Airport, Rome. This area has a typical Mediterranean climate with wet autumn and dry hot summer falling into the Koppen–Geiger class Csa (temperate, dry summer, hot summer) [60]. The average yearly maximum temperature is 27.4°C and the average minimum temperature is 5 °C. The average annual precipitation is 812 mm [61]. The soil in Maccarese is Cutanic Luvisol, with a prevailing sandy clay loam texture, becoming more clayey toward the north-east of the site.

The other site was located in Xiaotangshan (40.167° N, 116.4° E; 36 m a.s.l), Chanping district, Beijing, China. It is characterized by a continental climate, with a cold, dry winter and a hot, wet summer, belonging to the Koppen–Geiger [60] class Dwa (cold, dry winter, hot summer), i.e., monsoon-influenced, hot-summer humid continental climate. The soil in the experimental area was loam. The mean annual precipitation is approximately 602 mm. The mean temperature is approximately −4.5 °C in winter and 26.2 °C in summer. There are on average 180 frost-free days per year. The main crop is winter wheat. Table 2 shows sowing and harvest dates used for model simulations at the different test sites [38], which were set on the basis of local agronomic practice. Soil information for both the test sites is presented in Table 3.

Table 1. AOS parameters considered for sensitivity analysis with the range of values adopted in the present work.

Parameters Aquacrop v6.0 [a]	**AOS**	**Description**			**Unit**	**Range**
Management						
den	*PlantPop*	Plant population	n ha^{-1}	(2,000,000, 6,000,000)		
-	*PlantingDate*	Planting date	# Date	(736,965, 737,035)		
-	*HarvestDate*	Harvest date	# Date	(737,181, 737,250)		
Canopy development						
ccs	*SeedSize*	Soil surface area covered by an individual seedling at 90% emergence			cm^2	(1.05, 1.95)
-	*CCmin*	Minimum fractional canopy cover size below which yield formation does not occur			%	(0.04725, 0.08775)
mcc	*CCx*	Maximum fractional canopy cover size			%	(0.75, 1)
cdc	*CDC*	Canopy decline coefficient			fraction GDD	(0.0028, 0.0052)
cgc	*CGC*	Canopy growth coefficient			fraction GDD	(0.0042, 0.0078)
Phenology						
eme	*Emergence*	Thermal time from sowing to emergence			GDD [b]	(90, 230)
root	*MaxRooting*	Thermal time from sowing to maximum root development			GDD	(1200, 2011)
sen	*Senescence*	Thermal time from sowing to start of canopy senescence			GDD	(1090, 2250)
mat	*Maturity*	Thermal time from sowing to physiological maturity			GDD	(1590, 3150)
flo	*HIstart*	Thermal time from sowing to start of yield formation			GDD	(1090, 1395)
flolen	*Flowering*	Duration of flowering (thermal time)			GDD	(100, 300)
-	*YldForm*	Duration of yield formation (thermal time)			GDD	(770, 1430)
Transpiration, biomass and yield						
kcb	*Kcb*	Maximum crop coefficient when canopy is fully developed			-	(0.77,1.43)
kcdcl	*fage*	Decline of crop coefficient due to ageing of the canopy			$\%d^{-1}$	(0.21, 0.39)
wp	*WP*	Water productivity normalized for reference evapotranspiration and atmosphere carbon dioxide			g m^{-2}	(11, 22)
-	*Wpy*	Adjustment of water productivity parameter in yield formation stage			g m^{-2}	(75, 125)
-	*fsink*	Crop sink strength coefficient			-	(0.35,0.65)
hi	*HI0*	Reference harvest index			%	(0.32, 0.59)
-	*Hiini*	Initial harvest index			%	(0.007, 0.013)
hinc	*dHI0*	Maximum possible increase in harvest index above reference value			%	(0.1, 0.19)
exc	*exc*	Excess of potential fruits that is produced by the crop			%	(0.7, 1.3)

Table 1. *Cont.*

Parameters Aquacrop v6.0 [a]	AOS	Description	Unit	Range
Management				
Water and temperature stress				
-	*Tbase*	Base temperature below which crop growth does not occur	°C	(−1, −0.5)
-	*Tupp*	Upper temperature above which crop growth does not occur	°C	(18, 34)
polmx	*Tmax_up*	Maximum temperature above which pollination begins to fail	°C	(24, 45)
-	*Tmax_lo*	Maximum temperature above which pollination fails completely	°C	(28, 52)
polmn	*Tmin_up*	Minimum temperature below which pollination begins to fail	°C	(3, 6)
-	*Tmin_lo*	Minimum temperature below which pollination fails completely	°C	(−0.2, −0.1)
stbio	*GDD_up*	Minimum number of GDD's required for full biomass production	GDD	(9, 18)
-	*GDD_lo*	Minimum number of GDD's required for any biomass production to occur	GDD	(0, 5)
-	*fshape_b*	Shape factor describing the reduction in biomass production due to insufficient GDD's	-	(9.6694, 17.9575)
hipsflo	*dHI_pre*	Possible increase of harvest index due to pre-anthesis water stress	%	(0.02, 0.05)
hipsveg	*a_HI*	Coefficient describing the positive impact on harvest index of restricted vegetative growth post-anthesis	-	(1, 3)
hinsveg	*b_HI*	Coefficient describing the negative impact on harvest index of stomatal closure post-anthesis	-	(3, 6)
puexp	*p_up1*	Upper soil water depletion threshold for water stress effects on canopy expansion	fraction TAW [c]	(0.14, 0.26)
psto	*p_up2*	Upper soil water depletion threshold for water stress effects on stomatal control	fraction TAW	(0.455, 0.845)
psen	*p_up3*	Upper soil water depletion threshold for water stress effects on canopy senescence	fraction TAW	(0.49, 0.91)
ppol	*p_up4*	Upper soil water depletion threshold for water stress effects on crop pollination	fraction TAW	(0.595,1)
plexp	*p_lo1*	Lower soil water depletion threshold for water stress effects on canopy expansion	fraction TAW	(0.455, 0.845)
-	*p_lo2*	Lower soil water depletion threshold for water stress effects on stomatal control	fraction TAW	(0.7, 1)
-	*p_lo3*	Lower soil water depletion threshold for water stress effects on canopy senescence	fraction TAW	(0.7, 1)
-	*p_lo4*	Lower soil water depletion threshold for water stress effects on crop pollination	fraction TAW	(0.7, 1)
pexshp	*fshape_w1*	Shape factor describing water stress effects on canopy expansion	-	(2.1, 3.9)
pstoshp	*fshape_w2*	Shape factor describing water stress effects on stomatal control	-	(1.75, 3.25)
psenshp	*fshape_w3*	Shape factor describing water stress effects on canopy senescence	-	(2.1, 3.9)
-	*fshape_w4*	Shape factor describing water stress effects on crop pollination	-	(0.7, 1.3)
Soil and roots				
-	*REW*	User-defined readily evaporable water depth	m	(6.3, 11.7)
-	*CN*	Curve Number	-	(65, 85)
rtnx	*Zmin*	Minimum effective rooting depth	m	(0.15, 0.30)
rtx	*Zmax*	Maximum effective rooting depth	m	(1, 2.4)
rtexup	*SxTopQ*	Maximum water extraction at the top of the root zone	$m^3\ m^{-3}$ soil d^{-1}	(0.02, 0.03)
rtexlw	*SxBotQ*	Maximum water extraction at the bottom of the root zone	$m^3\ m^{-3}$ soil d^{-1}	(0.005, 0.01)

[a] as reported in [38,59]; [b] GDD: growing degree days; [c] TAW: total available soil water.

Table 2. Sowing and harvest dates for test sites.

	Maccarese, Italy		Xiaotangshan, China	
Period	**Sowing Date**	**Harvest Date**	**Sowing Date**	**Harvest Date**
2014–2015	1-Nov-14	1-Jul-15	-	-
2015–2016	8-Nov-15	30-Jun-16	7-Oct-15	19-Jun-16
2016–2017	10-Nov-16	15-Jul-17	1-Oct-16	10-Jun-17
2017–2018	30-Oct-17	28-Jun-18	15-Oct-17	30-Jun-18

Table 3. Soil conditions at study sites.

Maccarese, Italy									
Soil	**Depth (cm)**	**Moisture Content (%)**			**Organic C (%)**	**Clay (%)**	**Silt (%)**	**pH**	**Sand (%)**
		PWP	**FC**	**Sat**					
Sandy loam	0–10	8	18	45	2.4	33.3	19	6.6	47.8
Sandy loam	10–20	8	18	45	1.8	34.1	18.6	6.7	47.3
Sandy loam	20–30	8	18	45	1.8	33.6	20.4	6.7	46
Clay loam	30–40	18	23	43	1.8	34.6	19	6.7	46.4
Clay loam	40–50	18	23	43	1.5	32.4	17.8	6.8	49.8
Xiaotangshan, China									
Soil	**Depth (cm)**	**Moisture Content (%)**			**Organic C (%)**	**Clay (%)**	**Silt (%)**	**pH**	**Total N (%)**
		PWP	**FC**	**Sat**					
Clay loam	0–20	8.8	27.3	51.1	1.04	23.5	53.9	8.00	0.11
Clay loam	20–40	8.7	27.3	51.3	1.01	23.4	54.1	8.08	0.10
Clay loam	40–60	12.3	34.8	54.7	0.68	37.3	47.8	7.94	0.08
Clay loam	60–80	12.3	34.8	54.7	0.66	37.3	47.8	7.98	0.08
Clay loam	80–100	12.3	34.8	54.7	0.59	40.3	43	8.03	0.07

PWP: permanent wilting point; FC: field capacity; Sat: saturation.

2.5. Weather Data

Sensitivity analysis was carried out for four different wheat growth seasons (2014–2018) for the Maccarese site and for three seasons (2015–2018) for the Xiaotangshan site. The meteorological data used in this study to drive the model simulations for the SA were obtained from the Regione Lazio Agrometeorological Service, Italy (http://www.arsial.it/portalearsial/agrometeo/index.asp) and the National Meteorological Information Center of the China Meteorological Administration (http://cdc.cma.gov.cn/). The daily minimum and maximum temperatures, relative humidities, wind speed, rainfall data and daily solar radiation for the period were provided. The daily reference evapotranspiration was calculated based on the FAO Penman–Monteith method as described in [51] and the ET_0 calculator [62]. The minimum and maximum temperature, rainfall and reference evapotranspiration for both test sites are shown in Figure 1. For both sites, the years considered in this study allowed to include wet and dry conditions, which were assessed by examining the Standardised Precipitation-Evapotranspiration Index SPEI (https://spei.csic.es/index.html). In particular, the spring of 2017 was severely dry in Maccarese and also in Xiaotangshan, although for the latter the drought was limited to the month of May as shown in the Supplementary Materials (Figure S1).

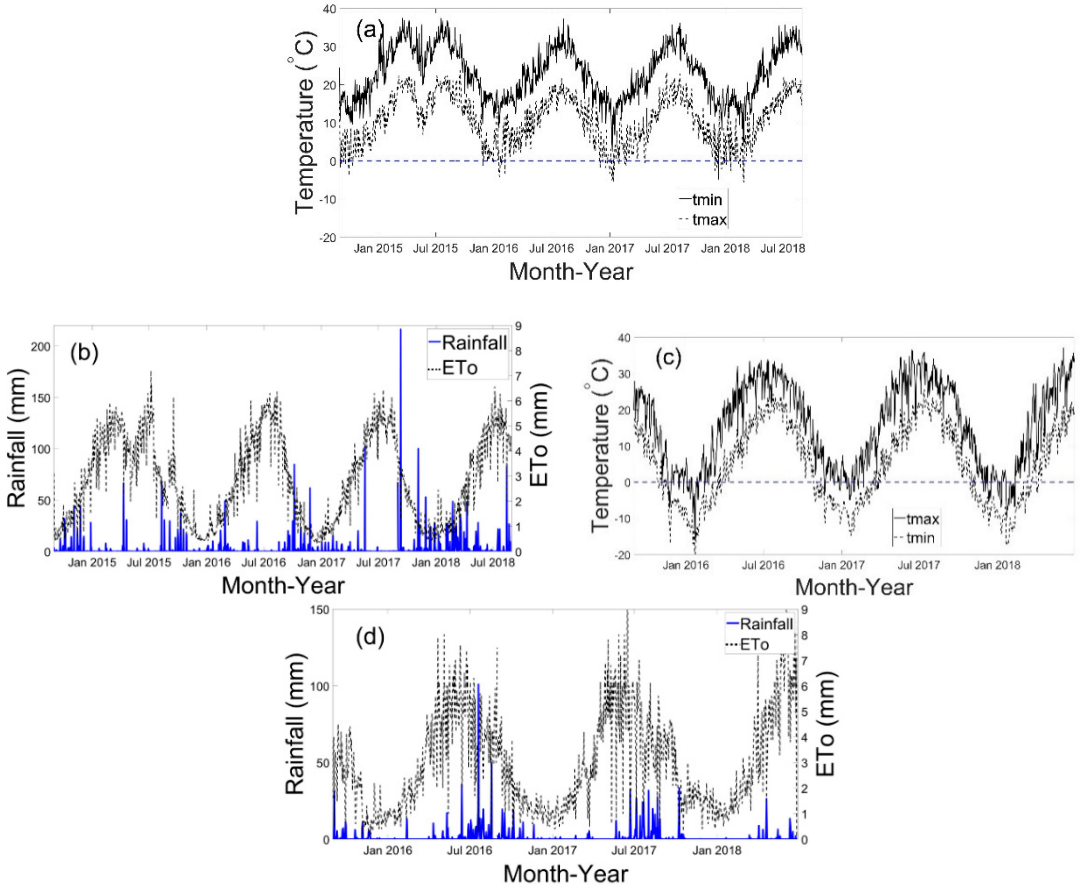

Figure 1. (**a**) Maximum and minimum temperature, (**b**) daily precipitation and reference evapotranspiration (ET_o) for Maccarese, Central Italy. (**c**) Maximum and minimum temperature, (**d**) daily precipitation and reference evapotranspiration (ET_o) for Xiaotangshan, China.

3. Results

3.1. Morris Method

Figure 2 shows the sensitivity of the AOS model parameters obtained by applying the Morris method for the two different locations, climates and years. In Figure 2, the average value for all the years is plotted, and the error bars indicate the variation (standard deviation) of the average value.

A large magnitude of μ^* indicates the importance of the model parameter. A high standard deviation of σ implies either a non-linear relationship or interaction with other parameters. The parameters *CGC* and *HIstart* were found to be of high importance for both the study sites regardless of the climate. The number of relevant parameters differs slightly for each year and study site. For the Maccarese site, 31 sensitive model parameters were identified for the years 2014–2015, 25 for 2015–2016, 23 for both the years 2016–2017 and 2017–2018. Similarly, for the Xiaotangshan site, 29 parameters were identified as most sensitive for 2014–2015, 29 for 2015–2016 and 23 for 2016–2017. When considering all years of data and study sites, 29 out of 55 (including dummy) were found important for yield output. These 29 parameters are plotted in Figure 2. For clarity purposes, only the parameters with the mean value of or greater than 1 $t\ ha^{-1}$ are labeled.

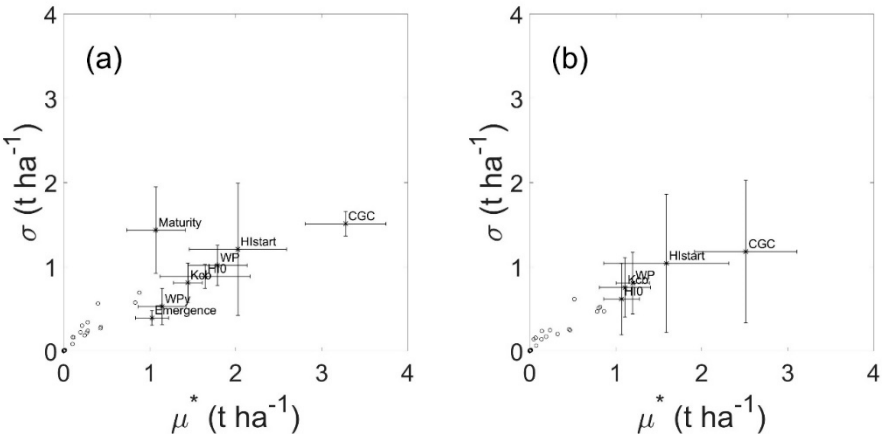

Figure 2. Morris method parameter screening results for (**a**) Maccarese and (**b**) Xiaotangshan test sites. Mean values of the Morris sensitivity indices μ^* and s are indicated by markers, and the errors bars indicate the standard deviation of index values across all the years. Only parameters with a μ^* value higher than 1 $t\ ha^{-1}$ are labeled. The meanings of parameter labels are reported in Table 1.

3.2. Variance-Based Extended Fourier Amplitude Sensitivity Test (EFAST)

Figure 3 shows the EFAST indices plots for all the parameters and all the years for the Maccarese test site. Both the first-order (S_i) and the total-order (St_i) indices are calculated, as proposed in [19], to distinguish between the main effect and the interaction effect.

For both study sites and all the years of weather data, the most relevant parameter was *CGC*, with the exception of 2016–2017 for both test sites; thus, this parameter is responsible for most of the variance of the output (Figures 3 and 4). The 2016–2017 season was particularly dry in Maccarese, with a three-month accumulated standardized precipitation-evapotranspiration index (SPEI) below −1 from February to July, indicating drought conditions (Figure S1). During that season, the parameter that resulted to have the highest sensitivity was *HIstart*. For Xiaotangshan test site (Figure S2), *Kcb*, *WP* and *HI0* were among the highest sensitive parameters after *CGC* for the years 2015–2016 and 2017–2018. During 2016–2017, *HIstart* had the highest sensitivity followed by *CGC*, *CDC*, *Kcb*, *WP* and *HI0*.

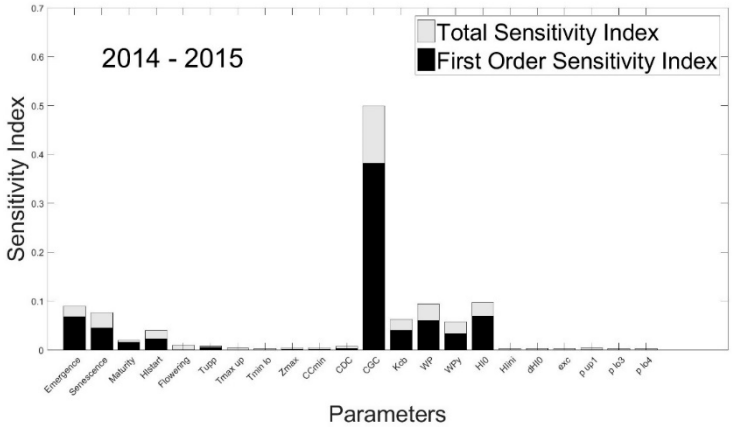

Figure 3. *Cont*.

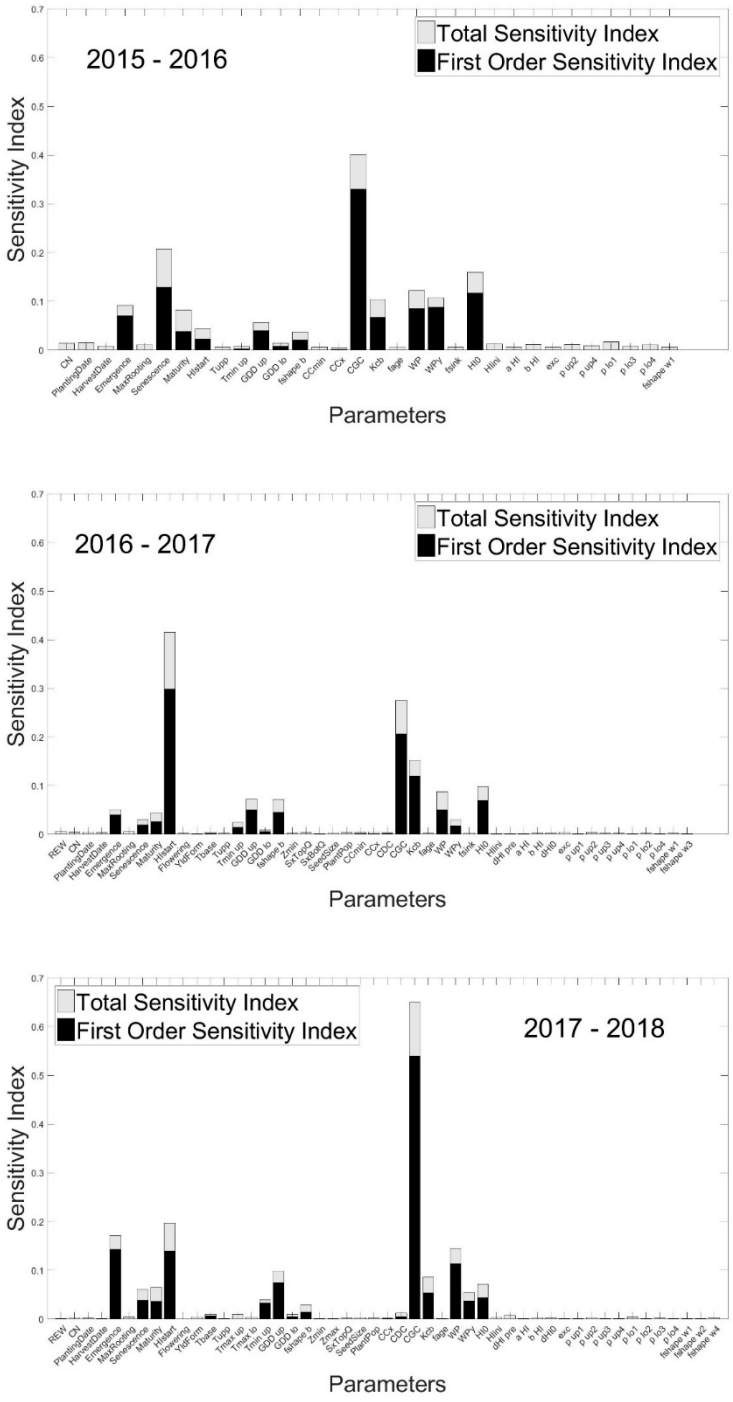

Figure 3. First-order and total-order SI for different years for Maccarese. Only the parameters with a total sensitivity index higher than the sensitivity index of the dummy parameter are shown. The details on the parameters can be found in Table 1.

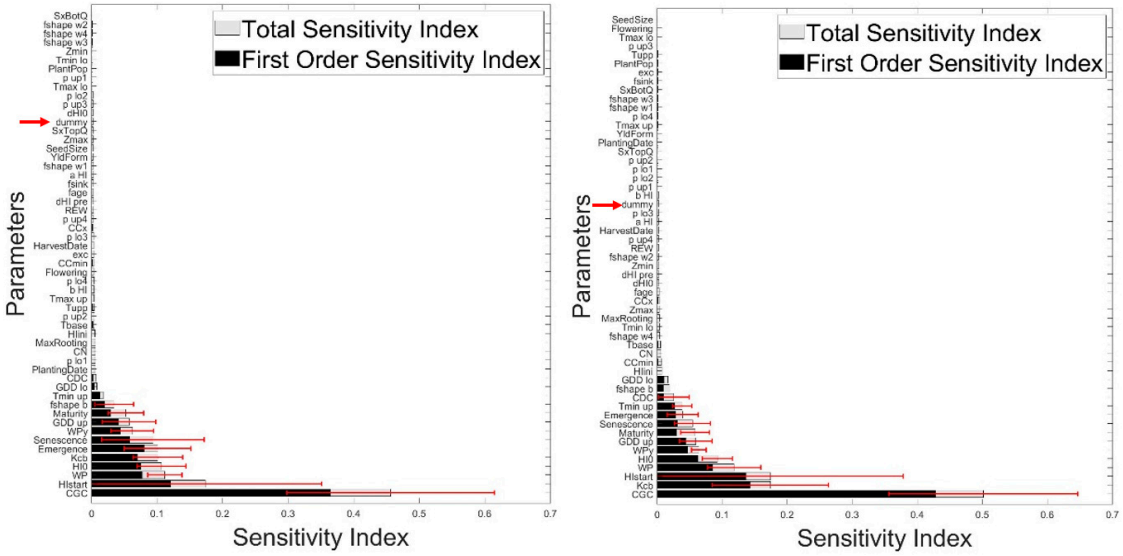

Figure 4. Average sensitivity indices using the EFAST method Maccarese (**left**) and Xiaotangshan (**right**) test sites. The error bars in red represent the extreme values of total-order sensitivity indices. The dummy parameter is highlighted with the red arrow.

The results of EFAST for winter wheat were quite similar for both study sites. Although, there were minor differences in the specific value of the St_i, and the general importance of the analyzed parameters was identical for both study sites. In the end, we used the average of the total sensitivity indices across all the years and study sites to find a similar set of sensitive parameters that could be adapted when calibrating AOS for regional studies (Figure 4).

The average indices for all the years are plotted in Figure 4, error bars indicating the extreme values for the total-order sensitivity indices. As expected, a small, but non-zero, value was estimated for the dummy parameter SI. For easy visualization and interpretation, the sensitivity indices are sorted in descending order. The parameters with SI values less than the SI of the dummy parameter were, thus, considered as non-influential parameters. The average SI for the Xiaotangshan location is shown in Figure 4.

3.3. Density-Based PAWN Method

Figures 5 and 6 show an example of two different obtained parameters with different and similar CDFs, illustrating the behavior of non-influential and influential parameters using the PAWN method. In Figure 5 it can be seen that for the parameter *CGC* the unconditional CDF and conditional CDF are different, and the value of the KS statistics is above the critical value at 95% confidence interval. Therefore, the model output has a high sensitivity to the parameter, which can be thus considered highly influential. On the contrary, Figure 6 shows an example of another parameter, *CDC*, with similar unconditional and conditional CDFs; the value of the KS statistic is below the critical value, and thus the parameter is non-influential and has a low SI.

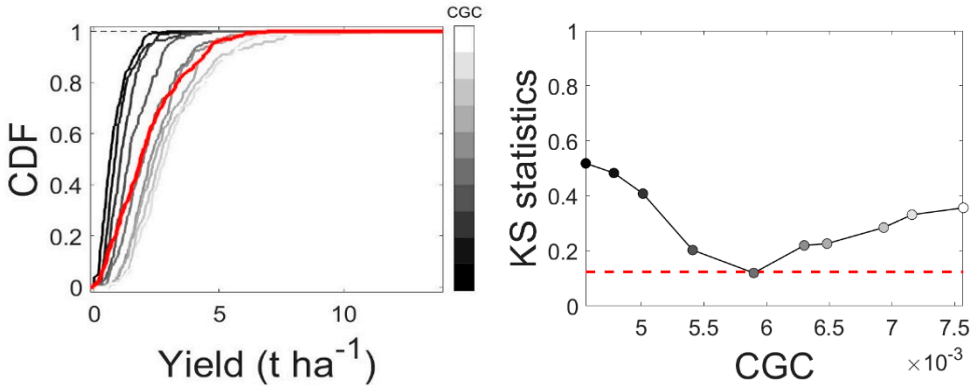

Figure 5. Cumulative Distribution Function (CDF) for the Canopy Growth Coefficient (CGC) parameter (**left**), red line on the left plot indicates the unconditional CDF and the grey colors represent the conditional CDF for ten different sampling points and Kolmogorov–Smirnov statistics (**right**), the red dashed line indicates the critical value of Kolmogorov-Smirnov (KS) statistics at 95% confidence interval.

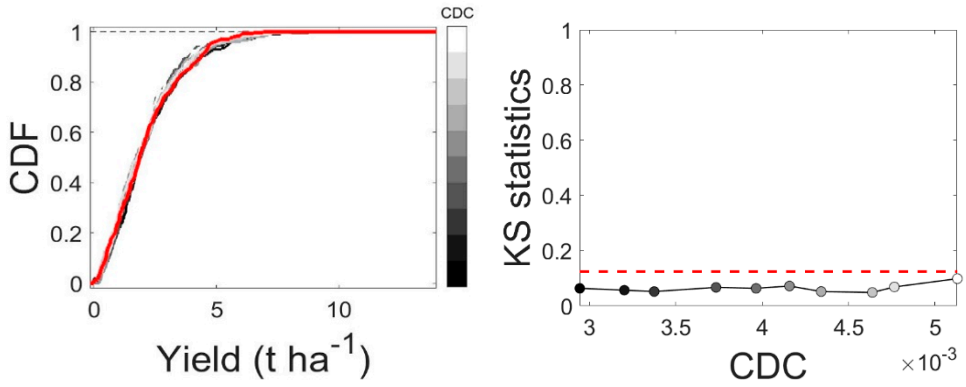

Figure 6. Cumulative Distribution Function (CDF) for the *CDC* parameter (**left**), red line on the left plot indicates the unconditional CDF and the grey colors represent the conditional CDF for ten different sampling points and Kolmogorov–Smirnov statistics (**right**), red dashed line indicates the critical value of Kolmogorov-Smirnov (KS) statistics at 95% confidence interval.

The PAWN index (T_i) for the different years is presented in Figure 7 for Maccarese and in Figure S3 (Supplementary Material) for Xiaotangshan. The average values of the indices for all the years are plotted in Figure 8, in which error bars represent the range of values for the PAWN sensitivity indices across the years. In comparison to EFAST, the sensitivity index appeared to be more stable. For both study sites, considering all the years of weather data, the most relevant parameter was *CGC*, also identified by EFAST method, and is also responsible for most of the variance of the model output. The second most influential parameter was *HIstart*. However, differently from EFAST, this parameter did not have a sensitivity index higher than CGC even in the water-stressed conditions of 2017. Again, as expected, a small but non-zero value was estimated for the SI of the dummy parameter. The parameters with the SI less than the SI of the dummy parameter are thus non-influential parameters. The average SI for the Xiaotangshan location is shown in Figure 8.

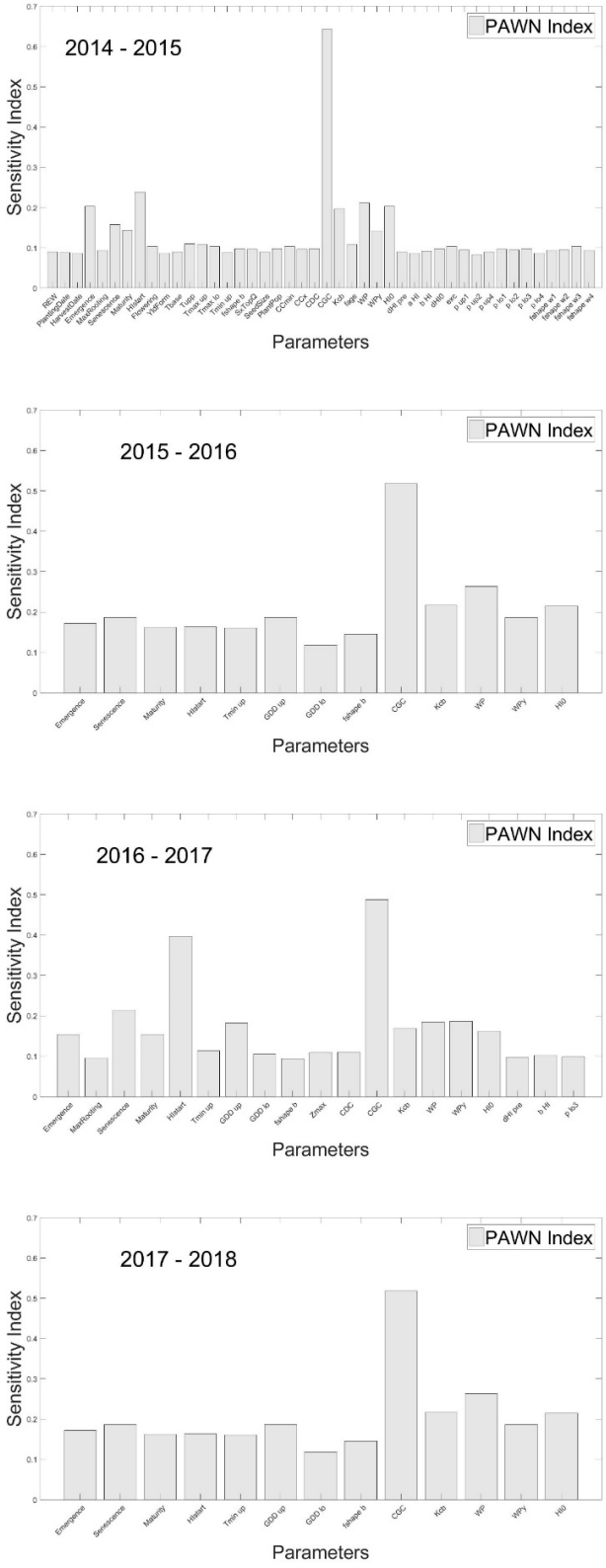

Figure 7. PAWN sensitivity index T_i for different years for the Maccarese location. Only the parameters with a total sensitivity index higher than the sensitivity index of the dummy parameter are shown. The details on the parameters can be found in Table 1.

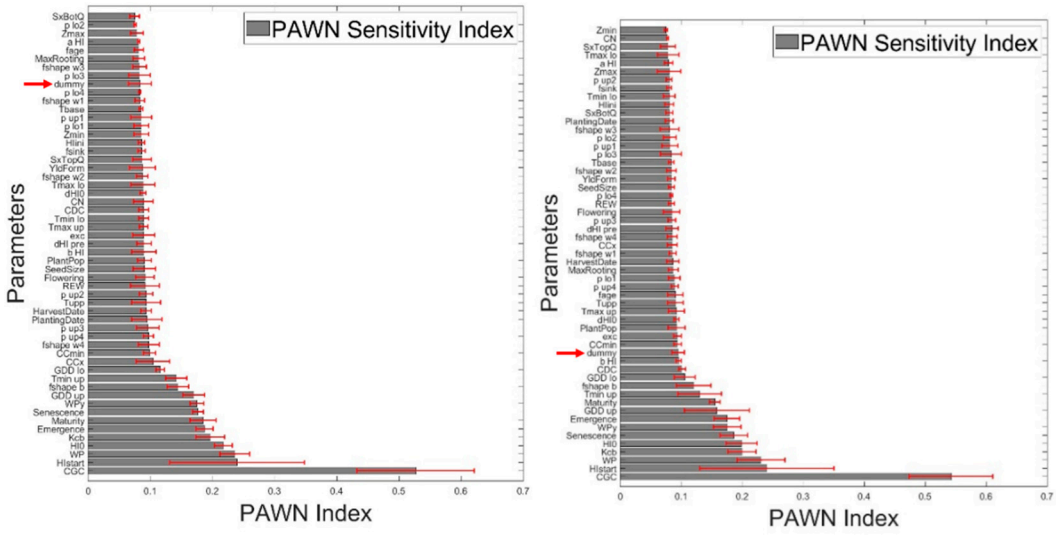

Figure 8. Average T_i using the PAWN method Maccarese test site (**left**) and Xiaotangshan test site (**right**). The error bars in red represent the extreme values of T_i. The dummy parameter is highlighted with the red arrow.

Identifying sensitive parameters using the PAWN method is suitable in the cases where the output distribution is not normal, and it follows skewed or multi-modal distribution [25]. An example of the output distribution is compared with 54 different statistical distributions. The top six best-fitted PDFs are mentioned in Table 4. The comparison is made on the basis of KS statistics and Anderson–Darling Statistics, with low values representing the best distribution. As can be seen, the Generalized Extreme Distribution has the lowest statistic value, with an Anderson–Darling statistic of 0.16401 and is second lowest in KS statistics. It is the best-suited PDF for the data, the reason for the choice of the PAWN method and is feasible to implement for identifying the most influential set of parameters for the local calibration. The Generalized Extreme Distribution is plotted in Figure 9, and statistics including the p-value and critical values at alpha (α) are presented in Table 5. The sample was from conditional CDF of the PAWN method, consisting of 200 samples, N_c = 200 (Section 2.1.3). It shows the statistics value and rank, indicating the raking of the distribution when compared with 54 PDFs (Table 4).

Table 4. Best probability distribution with Kolmogorov–Smirnov (KS) and Anderson–Darling statistics, ranking the best from top to bottom. Superscript in red indicates the rank of the KS and Anderson–Darling statistics.

Distribution	KS Statistics	Anderson–Darling Statistics
Gen. Extreme Values	0.03253 (2)	0.16401 (1)
Johnson SB	0.03047 (1)	0.19169 (2)
Gumbel Max	0.05197 (3)	0.4357 (3)
Logistic	0.12206 (4)	3.7302 (4)
Hypersecant	0.1276 (5)	4.0165 (5)
Normal	0.12242 (6)	4.0999 (6)

Similarly, for the Xiaotangshan test site, the most influential parameters are presented in Table 6, the descriptions of the parameters are mentioned in the list of AOS parameters (Table 1). The highly influential parameters for both the locations were *CGC*, *HIstart*, *WP*, *HI0*, *Kcb*, *Emergence*, *Senescence*, *WPy*, *GDD_up*, *Maturity*, *fshape_b*, *Tmin_up*, *GDD_lo*, and *CDC* (Figure 8 and Table 4).

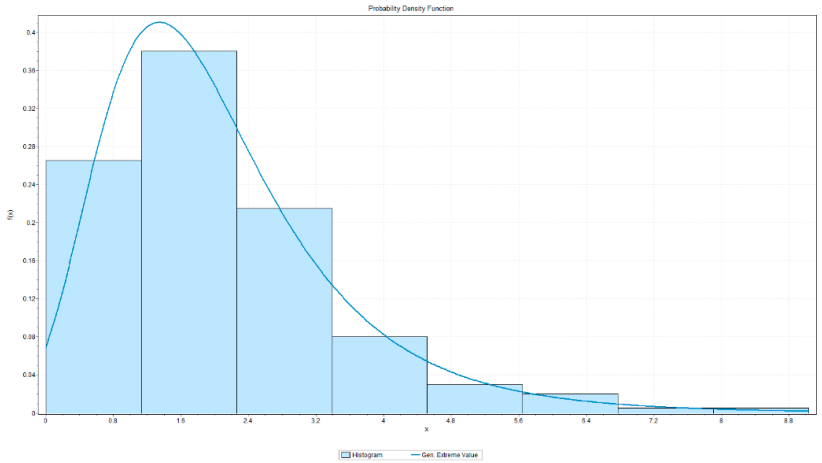

Figure 9. Generalized Extreme Values distribution fit to the output Yield from PAWN method.

Table 5. Best-fitted PDF (Generalized Extreme Values distribution) statistical summary.

Anderson–Darling Statistics					
Sample Size			200		
Statistics			0.16399		
Rank			1		
α	0.2	0.1	0.05	0.02	0.01
Critical Value	1.3749	1.9286	2.5018	3.2892	3.9074
Kolmogorov–Smirnov Statistics					
Sample Size			200		
Statistics			0.03251		
***P*-Value**			0.97963		
Rank			2		
α	0.2	0.1	0.05	0.02	0.01
Critical Value	0.07587	0.08648	0.09603	0.10734	0.11519

Table 6. List of sensitive parameters (based on the average SI values for all years) identified by different methods. Sorted in the decreasing order of the SI in the case of EFAST (Sti) and PAWN (Ti) method. The most influential parameters are in bold and underlined.

Study Site	Algorithm	Sensitive Parameters
Maccarese	Morris	***Emergence***, *Senescence*, ***Maturity***, ***HIstart***, *Tbase*, *Tupp*, *Tmax_up*, *Tmax_lo*, *Tmin_up*, *Tmin_lo*, *GDD_up*, *GDD_lo*, *fshape_b*, *Zmax*, *CCmin*, *CCx*, *CDC*, ***CGC***, ***Kcb***, *fage*, ***WP***, ***WPy***, ***HI0***, *HIini*, *exc*
	EFAST	***CGC***, ***HIstart***, ***WP***, ***HI0***, ***Kcb***, ***Emergence***, ***Senescence***, *WPy*, *GDD_up*, ***Maturity***, ***fshape_b***, ***Tmin_up***, ***GDD_lo***, ***CDC***, ***PlantingDate***, *p_lo1*, *CN*, *MaxRooting*, *HIini*, *T_base*, *p_up2*, *Tupp*, *Tmax_up*, *b_HI*, *p_lo4*, *Flowering*, *CCmin*, *exc*, *HarvestDate*, *p_lo3*, *CCx*, *p_up4*, *REW*, *dHI_pre*, *fage*, *fsink*, *a_HI*, *fshape_w2*, *YldForm*, *SeedSize*, *Zmax*, *SxTopQ*
	PAWN	***CGC***, ***HIstart***, ***WP***, ***Kcb***, ***HI0***, ***Senescence***, ***WPy***, ***Emergence***, ***GDD_up***, ***Maturity***, ***Tmin_up***, ***fshape_b***, ***GDD_lo***, ***CDC***, ***b_HI***
Xiaotangshan	Morris	*REW*, *Emergence*, *Senescence*, *Maturity*, ***Histart***, *Tbase*, *Tupp*, *Tmin_up*, *Tmin_lo*, *GDD_up*, *GDD_lo*, *fshape_b*, *Zmax*, *CCmin*, *CCx*, *CDC*, ***CGC***, *Kcb*, *fage*, ***WP***, *WPy*, ***HI0***, *exc*
	EFAST	***CGC***, ***Kcb***, ***HIstart***, ***WP***, ***HI0***, ***WPy***, ***GDD_up***, ***Maturity***, ***Senescence***, ***Emergence***, ***Tmin_up***, ***CDC***, ***fshape_b***,***GDD_lo***, ***HIini***, ***CCmin***, *CN*, *Tbase*, *fshape_w4*, *Tmin_lo*, *MaxRooting*, *Zmax*, *CCx*, *fage*, *HI0*, *dHI_pre*, *Zmin*, *fshape_w2*, *REW*, *p_up4*, *HarvestDate*, *a_HI*, *p_lo3*
	PAWN	***CGC***, ***HIstart***, ***WP***, ***HI0***, ***Kcb***, ***Emergence***, ***Maturity***, ***Senescence***, ***WPy***, ***GDD_up***, ***fshape_b***, ***Tmin_up***, ***GDD_lo***, *CCx*, *CCmin*, *fshape_w4*, *p_up4*, *p_up3*, *PlantingDate*, *HarvestDate*, *Tupp*, *p_up2*, *REW*, *Flowering*, *SeedSize*, *PlantPop*, *b_HI*, *dHI_pre*, *exc*, *Tmax_up*, *Tmin_lo*, *CDC*, *CN*, *dHI0*, *Tmax_lo*, *fshape_w2*, *YldForm*, *SxTopQ*, *fsink*, *HIini*, *Zmin*, *p_lo1*, *p_up1*, *Tbase*, *fshape_w1*, *p_lo4*

4. Discussion

4.1. Elementary Effects Using the Morris Method

The results obtained in this study, performed using a contrasting range of climatic scenarios of winter wheat growing areas in Maccarese, Italy (Mediterranean climate) and Xiaotangshan, China (continental climate), allowed to obtain essential information on the sensitivity of the AOS model, especially required for their application within regional-scale studies [63–65]. It is well known that the results of the sensitivity analysis studies depend on the boundary conditions chosen [66]. In this work, these conditions are climate datasets, actual data from both sites and the range of variation of the parameters [7,37,38]. The Morris method was used for initial screening of the parameters and to identify the influential and non-influential parameters. The influential parameters were found to be 29 for the Maccarese test site and 28 for the Xiaotangshan test site out of the total 54 model parameters considered in this study. These parameters are mentioned in Table 6, and the description of the parameters is reported in Table 1. A study [37] on the SA of the Aquacrop model used the mean value of 0.25 as a threshold, and parameters below 0.25 t ha^{-1} were classified as non-influential parameters. It was found that the parameters (translated in AOS notation) *exc*, *dHI0*, *p_up1*, *Tmin_up*, *Tmax_up*, *p_up4*, *SxTopQ* and *SxBotQ* were non-influential (<0.25 t ha^{-1}), and the other parameters *PlantPop*, *Flowering*, *HI0*, *dHI_pre*, *a_HI*, *Kcb*, *p_up2* and *fshape_w2* had low but non-negligible impacts (0.25–1.0 t ha^{-1}) for all the climatic scenarios implemented. In this study, the *CGC* parameter was found to be highly influential in all the conditions for both test sites. Another study carried out by [7] found almost the same parameter set of the non-influential parameters as by [37] in all the climatic conditions, with the exception of the soil curve number (*CN*) and the shape factor for water stress coefficient inducing early senescence (*fshape_w3*). It should be noted that the threshold considered in the study was 0.1 t ha^{-1} i.e., less than that used by [7]. The tabular comparison of the sensitive parameters is presented in Table 6.

4.2. Variance-Based Extended Fourier Amplitude Sensitivity Test (EFAST)

The Morris method is only used for initial screening, and it does not quantify the higher-order interaction between the parameters. This can be assessed by using the variance-based EFAST method and the density-based PAWN method for GSA. The comparison between these algorithms is not meaningful if compared on the basis of sensitivity indices as they have different rationales and backgrounds. This work applies a comparison based on the ranking of the parameters in both methods. So, to achieve this goal, all the input parameters, i.e., 55 including a dummy parameter, are used to carry out SA in both the methods.

Figure 3 shows both the first-order and the total-order sensitivity indices for the EFAST methods for all the years considered in this study. The sensitive parameters are, in general, common in all the climate years considered, but with different values of the SI. These common parameters are *Emergence, Senescence, Maturity, HIstart, CGC, Kcb, WP, WPy* and *HI0, Tmin_up, GDD_up* and *fshape_b*. The average sensitivity indices plots for all the years identify the non-influential parameters having a sensitivity less than the sensitivity of the dummy parameter. As can be seen from Figure 4, *dHI0, p_up3, p_lo2, Tmax_lo, p_up1, PlantPop, Tmin_lo, Zmin, fshape_w2, fshape_w3, fshape_w4* and *SxBotQ* had low sensitivities in comparison to the dummy parameter. These parameters are clearly identified as non-influential parameters.

Similarly, for the Xiaotangshan test site, the most influential parameters are reported in Table 6. The highly influential parameters for both the locations were *CGC, HIstart, WP, HI0, Kcb, Emergence, Senescence, WPy, GDD_up, Maturity, fshape_b, Tmin_up, GDD_lo* and *CDC* (Figure 4). These parameters are in common for both the test sites, although the ranking is not the same. Authors in [37] identified that for winter wheat in a temperate maritime climate, many parameters had an equivalent effect on the output variance, among which parameters describing canopy development were *SeedSize, CCx, CGC, Senescence*, *WP*, *GDD_up* and *Zmax*. In a previous study [7], it was found that the parameters

describing the phenological cycle of the crop and the water stress were among the most highly influential. The ranking of the parameters was different from that of [37], due to the climatic conditions employed. Also, the total-order effects were different than those of the first-order effects, indicating more complex higher-order interacting effects rather than individual effects. It should be noted that both these studies applied EFAST on the results of the Morris method, that is not the case of our study. The EFAST method for SA was directly applied to all the parameters in [38] under different irrigation treatments. In the presence of rainfall, *CGC*, *CCx*, *Emergence*, *PlantPop*, *SeedSize*, *Kcb*, *Maturity*, *Zmax*, *p_up3*, *MaxRooting*, *GDD_up* and *WP* were the most sensitive to yield. In normal irrigation, *CGC*, *CCx*, *Emergence*, *PlantPop*, *SeedSize*, *Kcb*, *Maturity*, *Zmax* and *p_up3* were among the highly influential, and in over-irrigation, *CGC*, *CCx*, *Emergence*, *PlantPop*, *SeedSize*, *Kcb*, *Maturity*, *Zmax*, *p_up3* and *CDC* were the most sensitive parameters. The translations of these parameters of Aquacrop and AOS model are mentioned in Table 1.

4.3. Density-Based PAWN Method

In the PAWN method, the sensitivity of the model output (yield) to the parameter x_i is measured by the distance between the conditional CDF of output obtained by fixing x_i, to a specific value and the unconditional CDF. Since all the variability related to x_i, both due to direct and interaction effects, is removed in the conditional CDF, the comparison illustrates the total effect of x_i. As a distance measure, the maximum absolute difference between two CDFs, i.e., the Kolmogorov–Smirnov statistic, is considered. The PAWN SI for the different years for Maccarese location is presented in Figure 7. The sensitive parameters are similar for all different years, but with a varying degree of the PAWN index. The average index for all the years is plotted in Figure 8. Table 6 summarizes the set of sensitive parameters based on the PAWN index.

The PAWN method is simpler and less computationally demanding in comparison to the EFAST method. Out of all the methods tested in this study, the Morris method was the simplest and required the lowest computational time, but the disadvantage with the method is that it does not quantify higher-order effects. The PAWN method, despite being simple, has two problems: first is the reliability of the CDF produced, which may become unstable as can be observed for both study sites. Fifteen parameters were identified as most influential for Maccarese study site, whereas 46 parameters appeared to have sensitivity higher than the sensitivity of the dummy parameter for the Xiaotangshan study site. However, the parameters with the highest sensitivity were in common for both the study sites. The other drawback of PAWN is the use of KS statistics to compute SI that leads to slow convergence.

4.4. Sensitive Parameters in Relation to Model Processes and Agronomic Conditions

AOS requires calibration of parameters to properly simulate crop growth, especially in new locations: SA can be used to identify the parameters that have the highest impact on crop yield, before proceeding to calibration. The interpretation of the SA results, in light of previously published literature and of the knowledge of model calculations and simulated processes, can provide useful insights for advanced as well as basic use of the model by researchers. Aquacrop parameters are divided into two main groups: conservative and non-conservative parameters. Conservative crop parameters do not change with time, cultivar, location nor water regime and in principle should require no adjustment to local conditions. If simulations do not match observed values, the first thing to look at is the fertility regime before changing the parameters. Non-conservative parameters, on the other hand, are dependent on the cultivar (e.g., phenology parameters) and conditions.

In our case, both in Maccarese and in Xiaotangshan, both methods (EFAST and PAWN) found *CGC*, *HIstart*, *WP*, *HI0* and *Kcb* to be the first five most sensitive parameters (Table 6), even though the order changed slightly between locations and methods. *CGC*, *WP*, *HI0* and *Kcb* are conservative parameters that showed a high impact on crop yield, while *HIstart* is a phenological non-conservative parameter. These parameters are mainly related to crop transpiration, which is directly used by AOS to calculate biomass accumulation (AOS is a water-driven model). *CGC* describes how fast the canopy cover (*CC*)

increases (Equation (7)). *CC* and *Kcb* are directly involved in the estimation of crop transpiration, which in turns determines biomass production through water productivity (*WP*). Grain yield is also highly influenced by the harvest index (*HI0*) and by the thermal time to start yield formation (*HIstart*). High fluctuations of yield estimations can therefore be expected when adjusting these parameters, and model users should be careful in this regard. Moreover, these parameters are also used to mimic the effects of fertility stress on crop growth in a semiquantitative way, since nutrient cycling is not directly incorporated into the model [59]. Testing parameter sensitivity under stress conditions is important for calibration purposes [67].

Other phenological parameters (e.g., *Emergence*, *Senescence* and *Maturity*) followed up in the SA with both locations and methods. Authors in [68] also included *Emergence* and *Maturity* as sensitive parameters for winter wheat cultivation in China, using the EFAST method. Authors in [7] found among the most influential parameters *Senescence*, *HIstart* and *Maturity* in winter wheat cultivated in a location in Central Italy (in the same region of Maccarese) and two locations in China (with Xiaotangshan being one of them). Similarly, authors in found *Emergency*, *Senescence* and *Maturity* to be among the highest influential parameters for winter wheat in Belgium. Authors in [38] also reported *HIstart* and *Maturity* among influential parameters for wheat cultivated near Beijing (using the EFAST method).

Water stress parameters (*p_up*, *p_lo* and *fshape_p*) are often the target of SA and calibration of Aquacrop. However, datasets for water-deficient conditions are usually needed to properly estimate the impact of these parameters on crop yield [69]. In this study, winter wheat was rainfed and not irrigated. Indeed, in the two locations considered, rainfall is frequent and evapotranspiration is low during the growing period (Figure 1), so it is not surprising that water stress parameters had lower sensitivity with respect to the canopy and phenological parameters for both locations and methods (Table 4). There are several examples that support this argument. Authors in [37] found water stress parameters to have a higher sensitivity order for winter wheat under drier conditions and more sandy soils. Authors in [33] simulated satisfactorily barley growth in southern Italy under rainfed conditions without the need to adjust water stress parameters for each year, while other crop growth and phenological parameters were specifically changed over the years. Authors in [70] obtained good simulations of winter wheat yield in Iran under moderate water stress without including water stress parameters in their SA and calibration. The SA carried out by [38] highlighted that the parameters with higher-order sensitivity to winter wheat yield in Beijing were mainly related to phenology, biomass accumulation and canopy growth, with *p_up3* (the threshold for water stress-related senescence) being the only water stress-related parameter included. In another recent global SA [59], maize water stress parameters were less sensitive than crop growth and phenology parameters, under all the irrigation treatments (designed to obtain a range of water stress intensities, from no to moderate stress). These experiences confirmed our results and highlighted that water stress parameters do not have high impact on winter wheat yield when water-limiting conditions are moderate.

5. Conclusions

In this paper, we compared the application of two global SA techniques, the variance-based EFAST and the moment-independent density-based PAWN method, to the analysis of 54 parameters of the AOS model, a crop growth simulation model widely used for canopy cover, biomass and yield simulations. With respect to the widely used variance-based sensitivity indices, the main advantage of PAWN is that it can be applied whatever the output distribution may be. The comparison was performed in terms of parameter ranking for different climates and geographical locations. In all the methods, highly influential parameters were common, and the ranking of these parameters was similar in EFAST and PAWN.

The PAWN method could be considered more adequate in our study, since the frequency distribution of the output variable was right-skewed. The use of a dummy parameter approach as a viable option to set a threshold value for parameter screening was demonstrated for all the methods

considered. The results reported in this study provide insight into identifying the most influential parameters of the AOS model for two different geographic locations with two different climates.

This set of most influential parameters can be used for model simplification and calibration of the most sensitive parameters. Simplification of the model is necessary for regional-scale studies and particularly for remote sensing data assimilation. Both EFAST and PAWN methods identified the most influential parameters for all different years for both the test sites, but with a varied sensitivity and ranking. According to the PAWN method, the highly influential parameters belonged to crop parameters specifically, to the canopy and phenological development (*CGC, HIstart, Senescence, maturity*), biomass/yield production (*WP, WPy*) and temperature stress (*Tmin_up, Tmin_lo, GDD_up*) rather than root development and water stress.

This study thus concludes that variance-based and density-based global SA methods are both useful, with the condition that the variance-based method should be preferable where a variance is an adequate proxy of the model output, i.e., where the model output distribution is normal. Although this work is limited to compare these two (EFAST and PAWN) methods on parameter ranking, for two different climates with seven years data overall, to verify the robustness of the comparison, it can be extended on the basis of efficiency, convergence or computational cost with other geographic locations, climates and crops.

Supplementary Materials: The following are available online at http://www.mdpi.com/2073-4395/10/4/607/s1, Figure S1: Standardised Precipitation-Evapotranspiration Index 3-months cumulative values trends for the Maccarese and Xiaotangshan sites for the periods used in the study (downloaded from https://spei.csic.es/index.html), Figure S2: First order and total order EFAST SI for different years for Xiaotansghan, Figure S3: PAWN sensitivity index Ti for different years for Xiaotansghan.

Author Contributions: D.U. implemented the methods, analyzed the data for the test sites and wrote the manuscript. R.C. supervised implementation and edited the manuscript. M.T. worked on the identification of the ranges of the parameters and edited the manuscript. S.P. (Simone Pascucci), S.P. (Stefano Pignatti), Z.L. and W.H. edited the manuscript. All authors have read and agreed to the published version of the manuscript.

Funding: This research was funded by the European Space Agency (ESA) and the Ministry of Science and Technology of China (MOST), under Dragon 4 Programme, Project ID32275-Topic1; it was also supported by the National Natural Science Foundation of China (418713339) and by the Italian National Research Council within the CNR-CAS Bilateral Agreement 2017–2019.

Acknowledgments: The authors gratefully acknowledge MIUR (Italian Ministry for Education, University and Research) for financial support (Law 232/216, Department of Excellence) to the DAFNE Department. The authors would like to thank the Maccarese Farm and the Region Lazio Agrometeorological Service, Italy, and National Meteorological Information Center of the China Meteorological Administration for proving weather data.

Conflicts of Interest: The authors declare no conflict of interest.

References

1. De Willigen, P. Nitrogen turnover in the soil-crop system; comparison of fourteen simulation models. In *Nitrogen Turnover in the Soil-Crop System*; Springer: Dordrecht, The Netherlands, 1991; pp. 141–149.
2. Hopmans, J.W.; Bristow, K.L. Current capabilities and future needs of root water and nutrient uptake modeling. *Adv. Agr.* **2002**, *77*, 104–175.
3. Gervois, S.; de Noblet-Ducoudré, N.; Viovy, N.; Ciais, P.; Brisson, N.; Seguin, B.; Perrier, A. Including croplands in a global biosphere model: Methodology and evaluation at specific sites. *Earth Interact.* **2004**, *8*, 1–25. [CrossRef]
4. Saltelli, A.; Tarantola, S.; Campolongo, F. Sensitivity anaysis as an ingredient of modeling. *Stat. Sci.* **2000**, *15*, 377–395.
5. Wallach, D.; Goffinet, B.; Bergez, J.-E.; Debaeke, P.; Leenhardt, D.; Aubertot, J.-N. Parameter estimation for crop models. *Agron. J.* **2001**, *93*, 757–766. [CrossRef]
6. Makowski, D.; Hillier, J.; Wallach, D.; Andrieu, B.; Jeuffroy, M. *Parameter Estimation for Crop Models. Working with Dynamic Crop Models*; Wallach, D., Makowski, D., Jones, J., Eds.; Elsevier: Amsterdam, The Netherlands, 2006; pp. 101–149.

7. Silvestro, P.C.; Pignatti, S.; Yang, H.; Yang, G.; Pascucci, S.; Castaldi, F.; Casa, R. Sensitivity analysis of the Aquacrop and SAFYE crop models for the assessment of water limited winter wheat yield in regional scale applications. *PLoS ONE* **2017**, *12*, e0187485. [CrossRef] [PubMed]
8. Yapo, P.O.; Gupta, H.V.; Sorooshian, S. Multi-objective global optimization for hydrologic models. *J. Hydrol.* **1998**, *204*, 83–97. [CrossRef]
9. Vrugt, J.A.; Bouten, W.; Gupta, H.V.; Sorooshian, S. Toward improved identifiability of hydrologic model parameters: The information content of experimental data. *Water Resour. Res.* **2002**, *38*, 48–61. [CrossRef]
10. Vrugt, J.A.; Gupta, H.V.; Bouten, W.; Sorooshian, S. A Shuffled Complex Evolution Metropolis algorithm for optimization and uncertainty assessment of hydrologic model parameters. *Water Resour. Res.* **2003**, *39*, 1–14. [CrossRef]
11. Pianosi, F.; Beven, K.; Freer, J.; Hall, J.W.; Rougier, J.; Stephenson, D.B.; Wagener, T. Sensitivity analysis of environmental models: A systematic review with practical workflow. *Environ. Model. Softw.* **2016**, *79*, 214–232. [CrossRef]
12. Duan, Q.; Sorooshian, S.; Gupta, V. Effective and efficient global optimization for conceptual rainfall-runoff models. *Water Resour. Res.* **1992**, *28*, 1015–1031. [CrossRef]
13. Bekele, E.G.; Nicklow, J.W. Multi-objective automatic calibration of SWAT using NSGA-II. *J. Hydrol.* **2007**, *341*, 165–176. [CrossRef]
14. Nossent, J.; Elsen, P.; Bauwens, W. Sobol' sensitivity analysis of a complex environmental model. *Environ. Model. Softw.* **2011**, *26*, 1515–1525. [CrossRef]
15. Wallach, D.; Makowski, D.; Jones, J.W.; Brun, F.; Jones, J.W. *Working with Dynamic Crop Models*; Academic Press: Cambridge, MA, USA, 2014; pp. 407–436.
16. Saltelli, A.; Ratto, M.; Andres, T.; Campolongo, F.; Cariboni, J.; Gatelli, D. *Global Sensitivity Analysis: The Primer*; John Wiley & Sons: West Sussex, UK, 2008.
17. Iooss, B.; Lemaître, P. A review on global sensitivity analysis methods. In *Uncertainty Management in Simulation-Optimization of Complex Systems*; Springer: Boston, MA, USA, 2015; pp. 101–122.
18. Chen, Y.; Cournède, P.-H. Data assimilation to reduce uncertainty of crop model prediction with convolution particle filtering. *Ecol. Model.* **2014**, *290*, 165–177. [CrossRef]
19. Saltelli, A.; Tarantola, S.; Chan, K.-S. A quantitative model-independent method for global sensitivity analysis of model output. *Technometrics* **1999**, *41*, 39–56. [CrossRef]
20. Cariboni, J.; Gatelli, D.; Liska, R.; Saltelli, A. The role of sensitivity analysis in ecological modelling. *Ecol. Model.* **2007**, *203*, 167–182. [CrossRef]
21. Sobol', I.M. On sensitivity estimation for nonlinear mathematical models. *Matem. Mod.* **1990**, *2*, 112–118.
22. Saltelli, A.; Chan, K.; Scott, M. *Sensitivity Analysis: Probability and Statistics Series*; John and Wiley & Sons: New York, NY, USA, 2000; pp. 3–14.
23. Van Griensven, A.V.; Meixner, T.; Grunwald, S.; Bishop, T.; Diluzio, M.; Srinivasan, R. A global sensitivity analysis tool for the parameters of multi-variable catchment models. *J. Hydrol.* **2006**, *324*, 10–23. [CrossRef]
24. Borgonovo, E. A new uncertainty importance measure. *Reliab. Eng. Syst. Saf.* **2007**, *92*, 771–784. [CrossRef]
25. Pianosi, F.; Wagener, T. A simple and efficient method for global sensitivity analysis based on cumulative distribution functions. *Environ. Model. Softw.* **2015**, *67*, 1–11. [CrossRef]
26. Saltelli, A. Sensitivity analysis for importance assessment. *Risk Analysis* **2002**, *22*, 579–590. [CrossRef]
27. Liu, H.; Chen, W.; Sudjianto, A. Relative entropy based method for probabilistic sensitivity analysis in engineering design. *J. Mech. Des.* **2006**, *128*, 326–336. [CrossRef]
28. Borgonovo, E.; Castaings, W.; Tarantola, S. Moment independent importance measures: New results and analytical test cases. *Risk Analysis: An International Journal* **2011**, *31*, 404–428. [CrossRef] [PubMed]
29. Zadeh, F.K.; Nossent, J.; Sarrazin, F.; Pianosi, F.; van Griensven, A.; Wagener, T.; Bauwens, W. Comparison of variance-based and moment-independent global sensitivity analysis approaches by application to the SWAT model. *Environ. Model. Softw.* **2017**, *91*, 210–222. [CrossRef]
30. Steduto, P.; Hsiao, T.C.; Raes, D.; Fereres, E. AquaCrop—The FAO crop model to simulate yield response to water: I. Concepts and underlying principles. *Agron J.* **2009**, *101*, 426–437. [CrossRef]
31. Foster, T.; Brozović, N.; Butler, A.P.; Neale, C.M.U.; Raes, D.; Steduto, P.; Fereres, E.; Hsiao, T.C. AquaCrop-OS: An open source version of FAO's crop water productivity model. *Agric. Water Manag.* **2017**, *181*, 18–22. [CrossRef]

32. Todorovic, M.; Albrizio, R.; Zivotic, L.; Saab, M.-T.A.; Stöckle, C.; Steduto, P. Assessment of AquaCrop, CropSyst, and WOFOST models in the simulation of sunflower growth under different water regimes. *Agron J.* **2009**, *101*, 509–521. [CrossRef]
33. Saab, M.T.A.; Todorovic, M.; Albrizio, R. Comparing AquaCrop and CropSyst models in simulating barley growth and yield under different water and nitrogen regimes. Does calibration year influence the performance of crop growth models? *Agric. Water Manag.* **2015**, *147*, 21–33. [CrossRef]
34. Xiangxiang, W.; Quanjiu, W.; Jun, F.; Qiuping, F. Evaluation of the AquaCrop model for simulating the impact of water deficits and different irrigation regimes on the biomass and yield of winter wheat grown on China's Loess Plateau. *Agric. Water Manag.* **2013**, *129*, 95–104. [CrossRef]
35. Jin, X.; Feng, H.; Zhu, X.; Li, Z.; Song, S.; Song, X.; Yang, G.; Xu, X.; Guo, W. Assessment of the AquaCrop model for use in simulation of irrigated winter wheat canopy cover, biomass, and grain yield in the North China Plain. *PLoS ONE* **2014**, *9*, e86938. [CrossRef]
36. Foster, T. *AquaCrop-OS v6.0a Reference Manual*; FAO: Rome, Italy, 2019.
37. Vanuytrecht, E.; Raes, D.; Willems, P. Global sensitivity analysis of yield output from the water productivity model. *Environ. Model. Softw.* **2014**, *51*, 323–332. [CrossRef]
38. Xing, H.; Xu, X.; Li, Z.; Chen, Y.; Feng, H.; Yang, G.; Chen, Z. Global sensitivity analysis of the AquaCrop model for winter wheat under different water treatments based on the extended Fourier amplitude sensitivity test. *J. Integr. Agric.* **2017**, *16*, 2444–2458. [CrossRef]
39. Morris, M.D. Factorial sampling plans for preliminary computational experiments. *Technometrics* **1991**, *33*, 161–174. [CrossRef]
40. Campolongo, F.; Cariboni, J.; Saltelli, A. An effective screening design for sensitivity analysis of large models. *Environ. Model. Softw.* **2007**, *22*, 1509–1518. [CrossRef]
41. Cukier, R.; Levine, H.; Shuler, K. Nonlinear sensitivity analysis of multiparameter model systems. *J. Comput. Phys.* **1978**, *26*, 1–42. [CrossRef]
42. Sobol, I.M. Sensitivity estimates for nonlinear mathematical models. *Mathematical modelling and computational experiments* **1993**, *1*, 407–414.
43. Kolmogorov, A. Sulla determinazione empirica di una lgge di distribuzione. *Inst. Ital. Attuari, Giorn.* **1933**, *4*, 83–91.
44. Smirnov, N.V. On the estimation of the discrepancy between empirical curves of distribution for two independent samples. *Bull. Math. Univ. Moscou* **1939**, *2*, 3–14.
45. Pianosi, F.; Sarrazin, F.; Wagener, T. A Matlab toolbox for global sensitivity analysis. *Environ. Model. Softw.* **2015**, *70*, 80–85. [CrossRef]
46. Ekstrom, P.-A. Eikos: A Simulation Toolbox for Sensitivity Analysis in Matlab. Master's Thesis, Uppsala University, Uppsala, Sweden, 2005.
47. Doorenbos, J.; Kassam, A. *FAO Irrigation and Drainage Paper No. 33 "Yield Response to Water."*; FAO–Food and Agriculture Organization of the United Nations: Rome, Italy, 1979.
48. Raes, D.; Steduto, P.; Hsiao, T.C.; Fereres, E. *AquaCrop-The FAO Crop Model to Simulate Yield Response to Water*; FAO Land and Water Division, FAO: Rome, Italy, 2009.
49. Tanner, C.B.; Sinclair, T.R. Efficient water use in crop production: Research or re-search? In *Limitations to Efficient Water Use in Crop Production*; American Society of Agronomy: Madison, WI, USA, 1983; pp. 1–27.
50. Steduto, P.; Hsiao, T.C.; Fereres, E. On the conservative behavior of biomass water productivity. *Irrig. Sci.* **2007**, *25*, 189–207. [CrossRef]
51. Allen, R.G.; Pereira, L.S.; Raes, D.; Smith, M. *Crop Evapotranspiration-Guidelines for Computing Crop Water Requirements-FAO Irrigation and Drainage Paper 56*; FAO: Rome, Italy, 1998; Volume 300.
52. Allen, R.G.; Pereira, L.S.; Raes, D.; Smith, M. *FAO Irrigation and Drainage Paper No 56*; Food and Agriculture Organization of the United Nations: Rome, Italy, 1998; Volume 56, p. e156.
53. Ritchie, J.T. Model for predicting evaporation from a row crop with incomplete cover. *Water Resour. Res.* **1972**, *8*, 1204–1213. [CrossRef]
54. McMaster, G.S.; Wilhelm, W. Growing degree-days: One equation, two interpretations. *Agric. For. Meteorol.* **1997**, *87*, 291–300. [CrossRef]
55. Raes, D.; Steduto, P.; Hsiao, T.; Fereres, E. *Chapter 1: FAO Crop-Water Productivity Model to Simulate Yield Response to Water: AquaCrop: Version 6.0-6.1: Reference Manual*; FAO: Rome, Italy, 2018.

56. Foster, T. Supplementary Information for 'AquaCrop-OS: An Open Source Version. Available online: https://ars.els-cdn.com/content/image/1-s2.0-S0378377416304589-mmc1.pdf (accessed on 22 April 2020).
57. Foster, T. *AquaCrop-OS v5.0a Reference Manual*; FAO: Rome, Italy, 2016.
58. Xing, H.; Li, Z.; Xu, X.; Feng, H.; Yang, G.; Chen, Z. Multi-Assimilation Methods Based on AquaCrop Model and Remote Sensing Data. *Transactions of the Chinese Society of Agricultural Engineering* **2017**, *33*, 183–192.
59. Guo, D.; Zhao, R.; Xing, X.; Ma, X. Global sensitivity and uncertainty analysis of the AquaCrop model for maize under different irrigation and fertilizer management conditions. *Arch. Agron. Soil Sci.* **2019**, 1–19. [CrossRef]
60. Peel, M.C.; Finlayson, B.L.; McMahon, T.A. Updated world map of the Köppen-Geiger climate classification. *Hydrol. Earth Syst. Sci. Discuss.* **2007**, *4*, 439–473. [CrossRef]
61. Upreti, D.; Huang, W.; Kong, W.; Pascucci, S.; Pignatti, S.; Zhou, X.; Ye, H.; Casa, R. A comparison of hybrid machine learning algorithms for the retrieval of wheat biophysical variables from sentinel-2. *Remote. Sens.* **2019**, *11*, 481. [CrossRef]
62. Raes, D. *The ETo calculator- Reference Manual*; FAO: Rome, Italy, 2012.
63. Casa, R.; Silvestro, P.; Yang, H.; Pignatti, S.; Pascucci, S.; Yang, G. Assimilation of remotely sensed canopy variables into crop models for an assessment of drought-related yield losses: A comparison of models of different complexity. In Proceedings of the 2016 IEEE International Geoscience and Remote Sensing Symposium (IGARSS), Beijing, China, 10–15 July 2016; pp. 5925–5928. [CrossRef]
64. Jin, X.; Li, Z.; Yang, G.; Yang, H.; Feng, H.; Xu, X.; Wang, J.; Li, X.; Luo, J. Winter wheat yield estimation based on multi-source medium resolution optical and radar imaging data and the AquaCrop model using the particle swarm optimization algorithm. *ISPRS J. Photogramm. Remote. Sens.* **2017**, *126*, 24–37. [CrossRef]
65. Silvestro, P.C.; Pignatti, S.; Pascucci, S.; Yang, H.; Li, Z.; Yang, G.; Huang, W.; Casa, R. Estimating Wheat Yield in China at the Field and District Scale from the Assimilation of Satellite Data into the Aquacrop and Simple Algorithm for Yield (SAFY) Models. *Remote. Sens.* **2017**, *9*, 509. [CrossRef]
66. Paleari, L.; Confalonieri, R. Sensitivity analysis of a sensitivity analysis: We are likely overlooking the impact of distributional assumptions. *Ecol. Model.* **2016**, *340*, 57–63. [CrossRef]
67. Jin, X.; Li, Z.; Nie, C.; Xu, X.; Haikuan, F.; Guo, W.; Wang, J. Parameter sensitivity analysis of the AquaCrop model based on extended fourier amplitude sensitivity under different agro-meteorological conditions and application. *Field Crop. Res.* **2018**, *226*, 1–15. [CrossRef]
68. Zhang, T.; Su, J.; Liu, C.; Chen, W.-H. Bayesian calibration of AquaCrop model for winter wheat by assimilating UAV multi-spectral images. *Comput. Electron. Agric.* **2019**, *167*, 105052. [CrossRef]
69. Abdalhi, M.A.M.; Jia, Z. Crop yield and water saving potential for AquaCrop model under full and deficit irrigation managements. *Ital. J. Agron.* **2018**, *13*. [CrossRef]
70. Salemi, H.; Soom, M.A.M.; Lee, T.S.; Mousavi, S.F.; Ganji, A.; Yusoff, M.K. Application of AquaCrop model in deficit irrigation management of winter wheat in arid region. *Afr. J. Agric. Res.* **2011**, *610*, 2204–2215.